CHAPTER 5

Alq_3-BASED SINGLE LAYER OLED WITH TPD:PBD BLEND THIN FILM

5.1 Doping Technology in OLED Fabrication

Doping method or more precisely blend method has been used in many fabrication of OLED especially for the solution-processed OLED [*Camurlu et al., 2009; Cossiello et al., 2008; S.-J. Kim et al., 2011; Reyes et al., 2004; Valadares et al., 2009; Yap et al., 2008, 2009*]. This solution process is easier and relatively low cost [*Hebner et al., 1998; Valadares, et al., 2009*] as compared to the other physical fabrication method, such as thermal evaporation technique. This process is also suitable for fabrication of a large area OLED especially through print-screen technique [*D. H. Lee et al., 2009*]. The performance of an OLED such as the turn on voltage [*W. J. Lee, Fang, Chiang, Ting, Chen, Chang, Lin, Lin, Wang, et al.*, 2003; *Xie et al.*, 2008] and the current and luminance efficiency [*Nie et al., 2007*] has been reported to improve when this method is applied to the OLED.

Usually, an electron transporting material is blended with a hole transporting material to promote a more balance carrier injection and transportation in the organic layer [*Chopra et al., 2008; Kao et al., 2011; Madasamy et al., 2008*]. Thus, this method is also implemented in an organic photovoltaic (OPV) cell to increase the fill factor (FF) and power efficiency [*Shih et al., 2011*]. Due to low mobility of hole, lanthanide

complexes such as europium and samarium are commonly blended with a hole transporting material, for instant, poly N-vinylcarbazole (PVK) to achieve a high mobility of hole [*J. Fang et al., 2006; Kin et al., 2008; Zhang et al., 2005*]. Another advantage of the blend technique is that the chemical and thermal properties of the materials can be significantly improved [*Costela et al., 2004*] and this is important especially in order to form a more stable thin film.

Due to excellent hole and electron transportation of TPD [*Kalinowski et al.*, 2008] and PBD [*C. E. Lee et al., 2001*], respectively, both materials have been used as host dopants for Alq_3 based OLED in this work. It is postulated that the blend device consists of Alq_3, TPD and PBD molecules will result in high luminance due to more electron and hole are transported in such device. Moreover, Alq_3 has a high glass transition (T_g) which is believed can stabilize the physical and thermal properties of TPD and PBD molecules which have low T_g in nature. This will also prevent the occurrence of crystallization process during the preparation of the blend thin film.

5.2 Experimental

Thin films of TPD, PBD and small molecule blends of TPD:PBD:Alq_3 were prepared by spin coating method as described in Chapter 3. The thickness of the thin films is about 80 nm. Clean glass was used as a substrate and the deposition was performed in low temperature of 25^{o}C, below Tg of organic materials to avoid crystallization of the films. A single layer OLED was constructed as ITO/PEDOT:PSS/Blend/Al where ITO and PEDOT:PSS act as the bulk anode layer, Alq_3-organic blend as the emissive layer and Al as the metal cathode. All samples were prepared in room temperature without encapsulation.

Structural properties were analyzed by FTIR (Perkin Elmer) and XRD (Siemens). Optical absorption and photoluminescence characteristics were obtained by UV-Vis-NIR (Jasco-V50) and luminescence spectrometer (Perkin Elmer LS 50B), respectively. The thickness of the thin film device was measured by profilometer (Tencor 6). Current density-voltage-luminance (*J-V-L*) characteristics were measured using chroma meter CS-200 (Konica Minolta) powered by source measure unit (Keithley 2400). Impedance measurements were carried out by using a Solatron 1260 Impedance analyzer. The amplitude of AC signal was 20 mV and the measurement frequency was set in the range of 10^{-1} Hz to 10^{-5} Hz. All characterizations of the device performance were performed at room temperature without encapsulation.

5.3 Optical and Photoluminescence Properties of TPD and PBD Thin Film

Initially, optical and PL properties of TPD and PBD thin film were investigated. Fig. 5.1 shows the normalized UV-Vis absorption spectra of TPD and PBD in thin film form taken at room temperature environment. The prominent absorption peaks for TPD and PBD are around 354 and 292 nm, respectively. Those peaks for TPD and PBD were found close to the ones previous reported in literatures by Vragovic et al. [*Vragović et al.*, 2008] and Paul et al. [*Paul et al.*, 2008] respectively. PBD has a very strong absorption at UV region (292 nm) corresponds to $\sigma \rightarrow \sigma^*$ band [*Paul, et al., 2008*] which indicates that it has a larger energy gap compared to that of TPD. Broad absorption peak from 300 to 400 nm can be observed for TPD molecule and it is attributed to $\sigma \rightarrow \sigma^*$, $\pi \rightarrow \pi^*$ and $\pi \rightarrow$d electronic transitions. The broad absorption peak of TPD molecule indicates a disorder arrangement in molecular level of the organic molecule.

In order to determine the value of an optical energy gap, graphs of $(\alpha h\nu)^2$ against E were plotted, as shown in Fig 5.2. α, h and ν is the absorption coefficient, Planck

constant and frequency, respectively. Extrapolation of the plot at $(\alpha h\nu)^2 = 0$ gives the optical energy gap, E_g. From Fig 5.2, the presence of a direct allowed transition of TPD, and PBD thin film were obtained with energy gaps of 3.12±0.02 eV and 3.50±0.02 eV, respectively. The energy gaps value obtained for TPD and PBD are almost the same as reported by J.-H. Lee [*J.-H. Lee et al.*, 2000] and An et al. [*An et al.*, 1998] respectively. Therefore, the typical energy band diagram of TPD and PBD can be illustrated as Fig. 5.3.

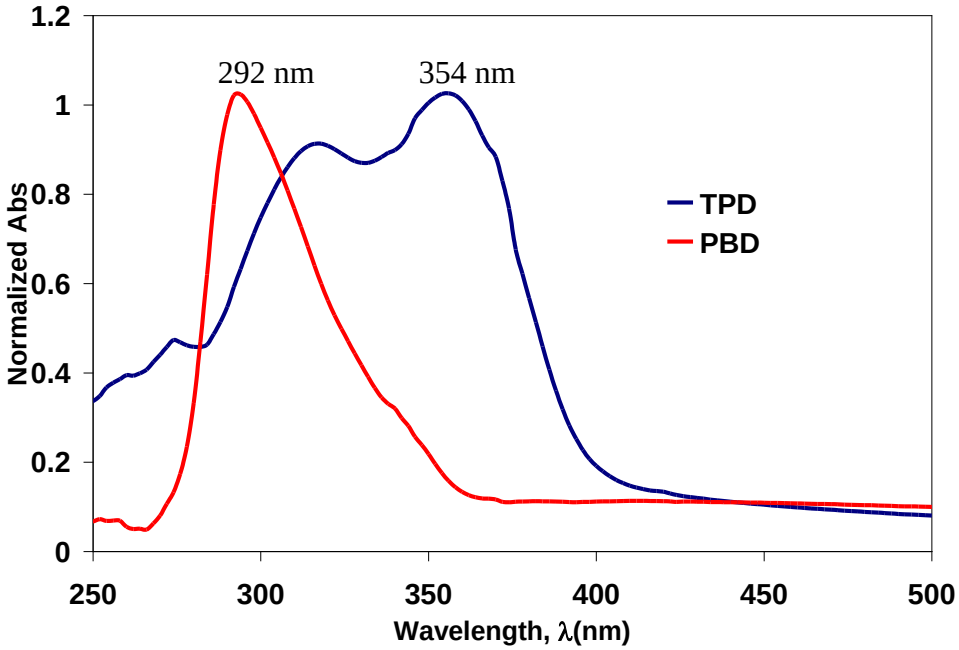

Figure 5.1: Normalized UV-Vis absorption of TPD and PBD in thin film form. The spectra were normalized with respect to the highest absorption intensity for each material

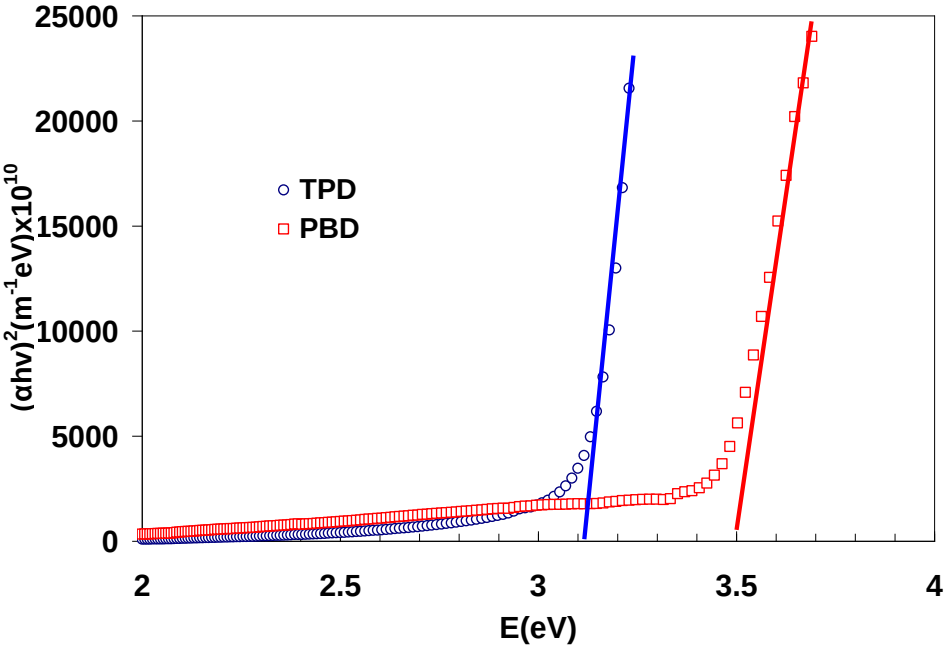

Figure 5.2: $(\alpha hv)^2$ vs E plot of TPD and PBD

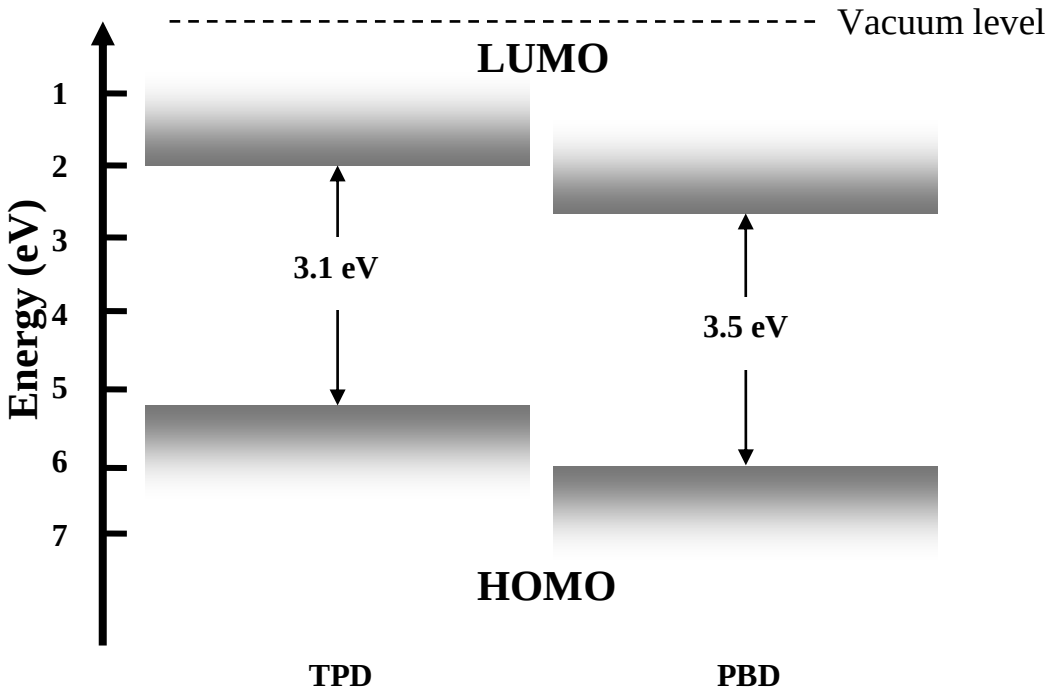

Figure 5.3: A typical molecular energy level of TPD and PBD

It is essential to study the luminescence properties of the materials in order to fabricate good OLED devices. For that purpose, photoluminescence (PL) was performed to the samples. From the absorption results, the absorption edges wavelengths are used as excitation wavelength in PL experiment. For the host materials, 280 nm excitations line has been selected. This is because excitation line can cover energy ranges of both materials such that the electron from the ground state can jump to the excited state. The normalized PL spectra of the TPD and PBD in the thin film form are shown in Fig. 5.4. The PL peak for TPD and PBD are centered at 415 and 374 nm, respectively. The PL spectra of the films show a significant red-shift behavior from the absorption spectra which follow Franck-Condon transitions that state the emission energy must be less than the excitation energy. This is also known as Stoke's shift phenomenon. The results show that the emission from the hosts is in the blue spectrum range and has a tail broadening towards the red color region. These PL emission peaks of TPD and PBD were found to be closed to the value the was published by Tsuboi et al. [*Tsuboi et al.*, 2009] and Paul et al. [*Paul, et al.*, 2008], respectively. The strong emission in the blue color region is attributed to $S_1(0)$-$S_0(v)$ fluorescence emission where S_0 and S_1 is the ground state and the first singlet state of an electronic vibration, respectively, with respect to frequency, v. The weak emission spectrum at a higher wavelength corresponds to $T_1(0)$-$S_0(v)$ phosphorescence emission where T_1 is the triplet state of an electronic vibration. It is noted that the fluorescence emission occur much faster than that of the phosphorescence emission due to a shorter energy transfer pathway. A high probability of relaxation occur at the transition from $S_1(0)$-$S_0(v)$, and the energy gap of the transition is larger than that from $T_1(0)$-$S_0(v)$, thus most of the emission from the small molecules occurred at a low wavelength in the blue region. Schematic diagram of the photoluminescence mechanism is shown previously in Fig. 2.4, Chapter 2.

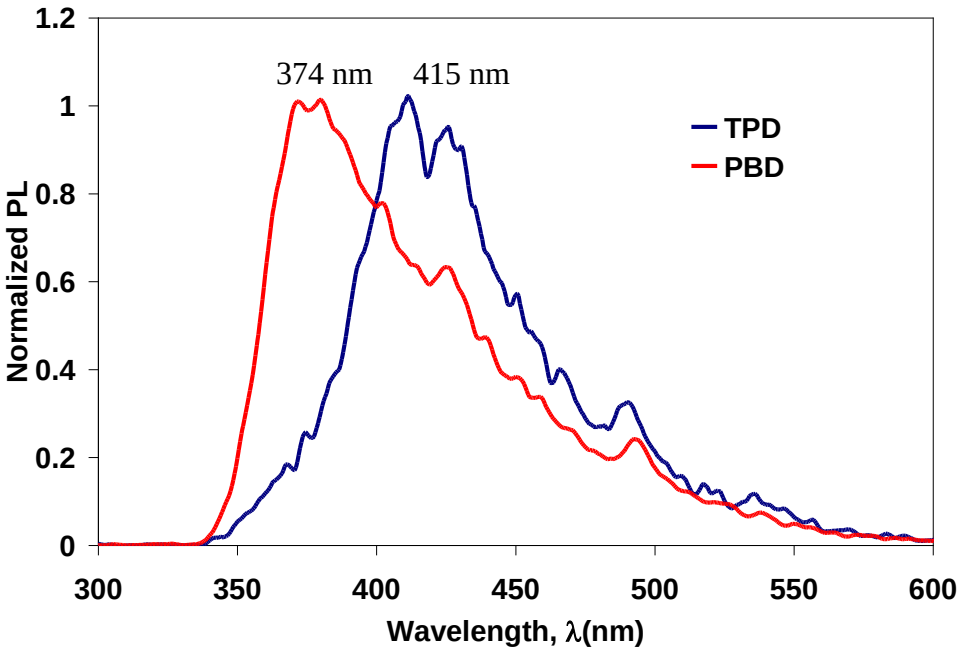

Figure 5.4: Normalized PL spectra of TPD and PBD in thin film form excited under 280 nm excitation energy.

5.4 Structural Properties of Alq_3 Doped TPD:PBD Blend Thin Film

Fig. 5.5 shows the normalized FTIR transmittance of Alq_3, TPD, PBD and the blend of TPD:Alq_3 and TPD:PBD:Alq_3 in thin film form in the range from 800 to 2000 cm^{-1} of wavenumber. The transmittance spectrum of TPD:PBD:Alq_3 blend shows the significant overlap from each vibration mode of TPD, PBD and Alq_3 molecules. Finger print of Alq_3 molecule at wavenumber of 1460 and 1500 cm^{-1} are observed to be broader in the blend system due to a large overlapping of the vibration peak at 1480 cm^{-1} which is due to the protonated quinoid ring stretching mode [*Hopkins et al., 2004*] of TPD and PBD molecules. The overlapping of these conjugated rings may leads to an enhancement of carrier transportation process where the free charge carrier can easily passes through the backbone among the small molecules in such a blend system when an electric field is applied. Stretching mode band of C-O at around 1210 to 1320 cm^{-1} of TPD and PBD molecules are observed to overlap with a CH/CCN bending and CN stretching vibrations, thus broadening the peaks for the blends films of TPD:Alq_3 and TPD:PBD:Alq_3.

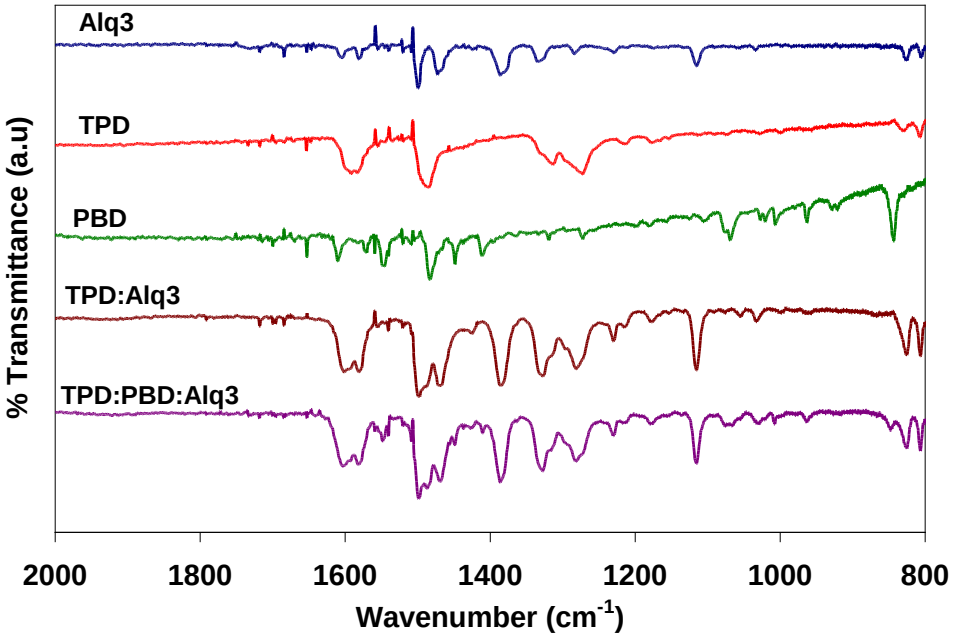

Figure 5.5: FTIR spectrum of the small molecules and their blends in the wavenumber range from 800 to 2000 cm^{-1}.

Fig. 5.6 shows the XRD pattern of Alq_3, TPD, PBD and the blend of TPD:Alq_3 and TPD:PBD:Alq_3 in thin film form. All peaks exhibit a broad XRD peak in the range of 15 to 40^o which is related to the disorder molecular structure of an amorphous thin film. The spectra show no significant crystal peak in all range of angle indicating that the nature of the molecules and their blends are pure amorphous in solid state form. Small peaks observed in all spectrums are assigned as noise of the XRD pattern. The similar amorphous property of XRD pattern was reported to be obtained from small molecule deposited by thermal evaporation technique, however the structural organization turn to crystalline form as the thin film was annealed at 200^{o}C for 2 hours [*El-Nahass et al., 2010*].

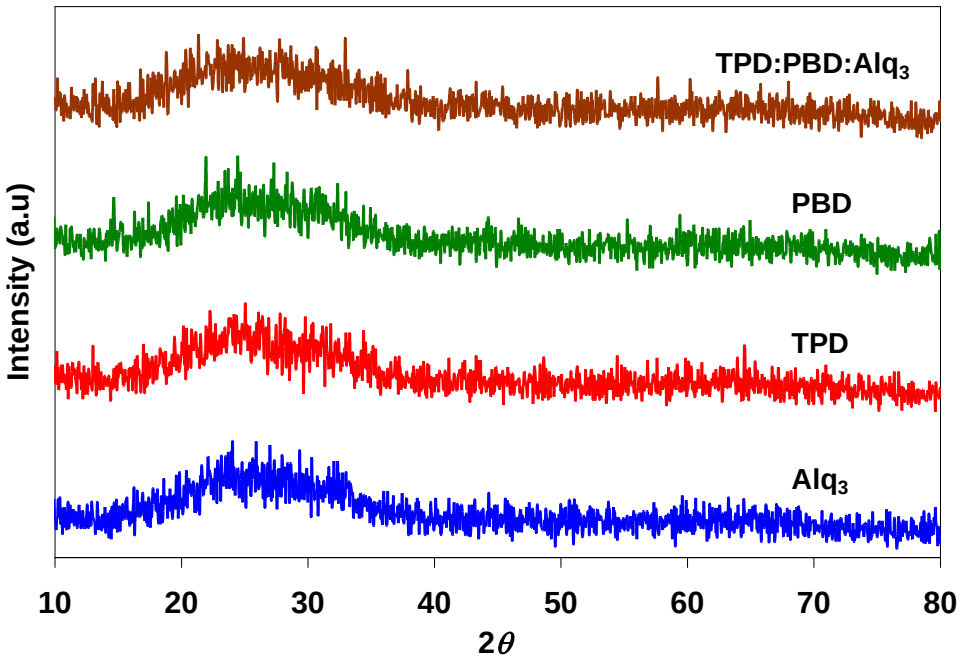

Figure 5.6: XRD pattern of Alq_3, TPD, PBD and blend of TPD:Alq_3 and TPD:PBD:Alq_3 in thin film form.

5.5 Optical and Photoluminescence Properties of Alq_3 Doped TPD:PBD Blend Thin Film

Fig. 5.7 shows the normalized UV-Vis absorption spectra for the different blend systems measured in the thin film form. Three different absorption spectra observed are strongly related to their dopant molecules. The maximum absorption peak for the pure Alq_3 is obtained at 386 nm while for TPD:Alq_3 and TPD:PBD:Alq_3 blend thin films, the maximum absorption peak is observed shifted towards lower wavelength of 354 and 308 nm, respectively. The spectra are expected to show the identical absorption peak for each component due to almost zero electronic molecular interaction between each material at the ground state level. The basic structure for the molecular level of each component of the blend should remain the same as the pure material. It can be observed that the absorption peak of the blend system is dominated by the absorption of the dopants material probably related to the strong absorption intensity of the dopants that overlaps with the absorption spectra of Alq_3. For the TPD:PBD:Alq_3 blend system, the absorption peak of oxadiazole moieties is observed in the range of 275–350 nm as

similarly reported by Xu et al. [*Xu et al.*, 2006]. This indicates that the oxygen and nitrogen atoms in the oxadiazole moiety are tidily bonded and do not form a coordinate bond with the aluminum from Alq_3 molecule.

Tauc relation has been used to determine the energy gap of the blend thin films. Fig. 5.8 shows the $(\alpha hv)^2$ vs E plot of the blend thin film with the value of n = ½. From the Tauc plot, the energy gap of Alq_3, TPD:Alq_3 and TPD:PBD:Alq_3 thin films are obtained with the value of 2.79± 0.02 eV, 3.05±0.02 eV and 3.15±0.02 eV, respectively. There is a significant increase in the energy gap as the dopant are added to the blend system. This indicates that the increase in the energy gap is strongly related to the dopant system. In particular in the TPD:PBD:Alq_3 blend film, absorption of σ→σ* electronic transition is dominant as compared to that of absorption from π→π*, which is assigned to strong N-H and O-H single bond of PBD dopant.

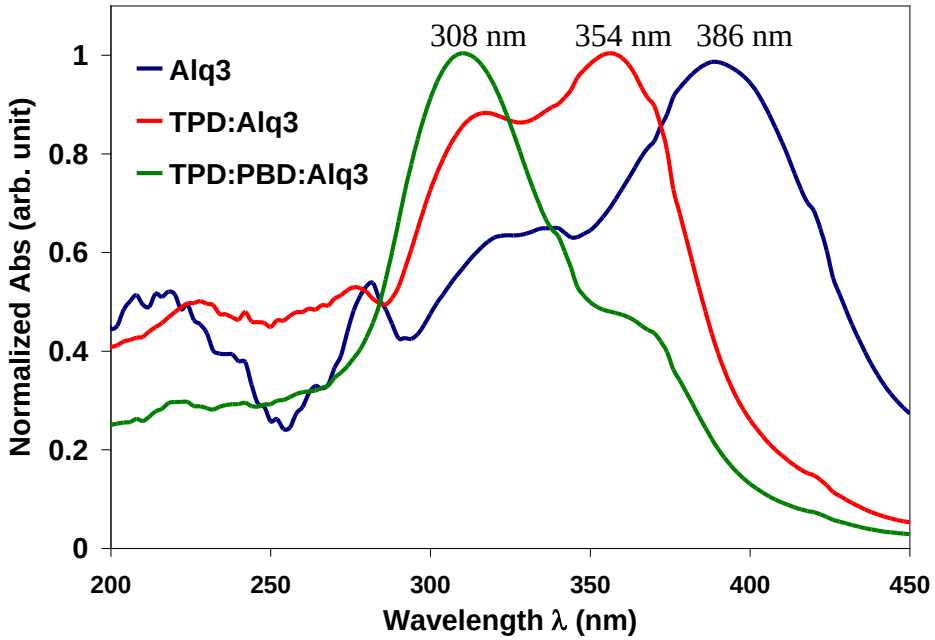

Figure 5.7: Normalized UV-Vis absorption of blend in thin film form

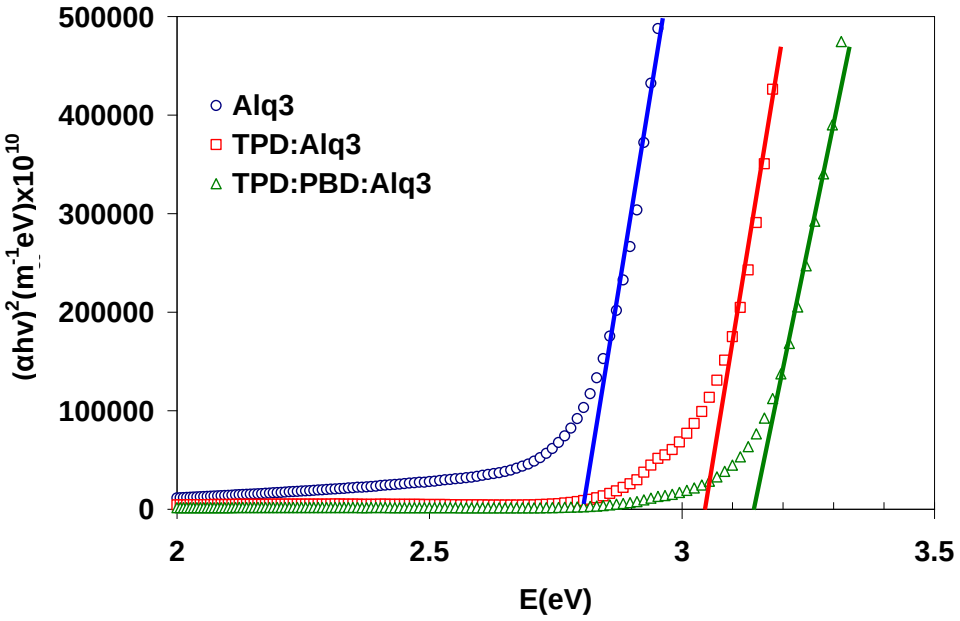

Figure 5.8: $(\alpha hv)^2$ vs E plot of blend thin film

PL measurement of the blend thin films were investigated under 312 nm excitation wavelength and the PL spectra is shown in Fig. 5.9. These PL spectra show interesting properties in which the intensity increases with the increase in the dopant added to the system. However, the PL peaks position for such blend remains almost at the same wavelength of 516 nm. These PL results can be related to the efficient energy transfer from host to guest, where TPD and PBD is the host and Alq_3 is the guest. A high energy gap in the blend thin films allows the hosts to absorb more photon energy and transfer them efficiently to the guest Alq_3. This energy transfer is the irradiative type of an internal conversion and it occurs from host to guest molecule. The transferred energies in Alq_3 molecular level is then excited the electrons in its HOMO level. These excited electrons recombined with holes in the relaxation process which releases PL emission. Thus, the emission only occurs at Alq_3 guest, and not TPD and PBD host. Similar agreement has been reported by Neghabi et al. [*Neghabi et al.*, 2012] where ternary OLED system of TPD:Alq_3:C_{60} has been fabricated and studied. The summary of the optical and PL properties of the blend film are tabulated in Table 5.1.

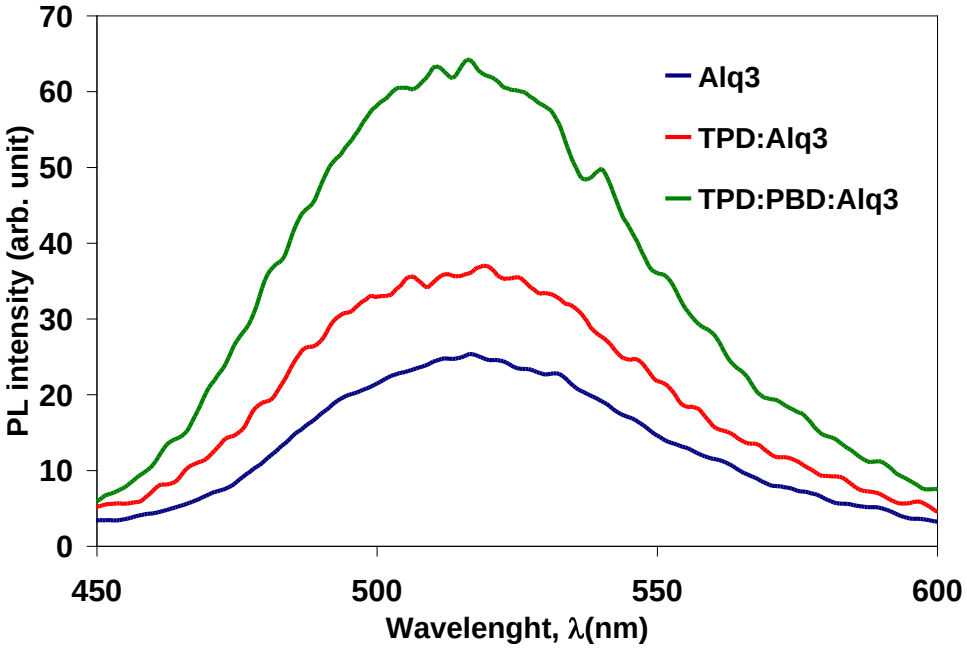

Figure 5.9: PL intensity of blend in thin film form with excitation wavelength of 312 nm

Table 5.1: Summary of optical and PL properties of the blend films.

	Thin films				
	Alq_3	TPD	PBD	TPD:Alq_3	TPD:PBD:Alq_3
Abs, λ_{max} (±1 nm)	392	352	292	356	310
PL, λ_{max} (±1 nm)	516	412	308	516	516
Eg (±0.02 eV)	2.80	3.12	3.50	3.05	3.15

5.6 Performance of Single Layer OLED

Single layer OLEDs are fabricated based on ITO/PEDOT-PSS/Blend thin film/Al configuration. The hetero structure of Indium tin oxide (ITO) and PEDOT-PSS is the transparent anode, the blend thin film is the emission layer and aluminum metal is set as the cathode. The electrical properties of the OLEDs devices were tested in room temperature without encapsulation. The current density-voltage (*J-V*) characteristics of the single layer OLEDs are shown in Fig. 5.10. Obviously, the current density of OLEDs increases with the increase in the doping elements in the blends emissive layer. This provide the evident that the doping method enhances the mobility of the OLED as reported in ref. [*Blochwitz et al., 1998*]. The critical voltage of the Alq_3 OLEDs (more than 20 V) is significantly reduced for the TPD:PBD:Alq_3 OLEDs (11.5V). Above this

voltage, the luminance decreases with the increase in the voltage, indicating that the OLEDs have degraded due to the high electric field and Joule heating [*Adachi et al., 1990*].

The injection properties of the devices were investigated by employing Fowler-Nordheim (FN) plot. Assuming the injection mechanism of the devices follows the theory of FN tunneling, graphs $\ln(J/F^2)$ versus 1/F were plotted in order to study the hole injection mechanism. Fig. 5.11 shows the FN plot of the OLED with different doping system. Gradient of the linear fitting gives information on the effective barrier height. The calculated effective hole injection barrier indicates that the barrier height is reduced significantly from 0.88±0.05 eV for pure Alq_3 to 0.39±0.05 eV for TPD:PBD:Alq_3 device. The reduction in the hole barrier height facilitates the injection of hole from the anode to the organic layer. M. Neghabi et al. [2012] has report that the injection barrier for the similar device of TPD:Alq_3 is 0.11 eV, which is lower than that obtained from the fabricated device in this study. Such discrepancy is due to the different blend ratio. In their case, they used the TPD:Alq_3 blend ratio of 10:2, which believe cause a significant reduction of barrier height. These results explained the significant improvement in the turn-on voltage of the blended OLED. Thus, it is highly believed that the mobility carrier of the device was increased by blending the Alq_3 molecule with the TPD and PBD molecules. Based on the improvement in the carrier injection property, the injected carriers travel through the organic blend thin film with a higher mobility which results in an increase in the current density. A high current density accumulation in such an organic blend may cause heat to increase and thus explain the occurrence of Joule heating phenomena in the lower driven voltage for the blend devices.

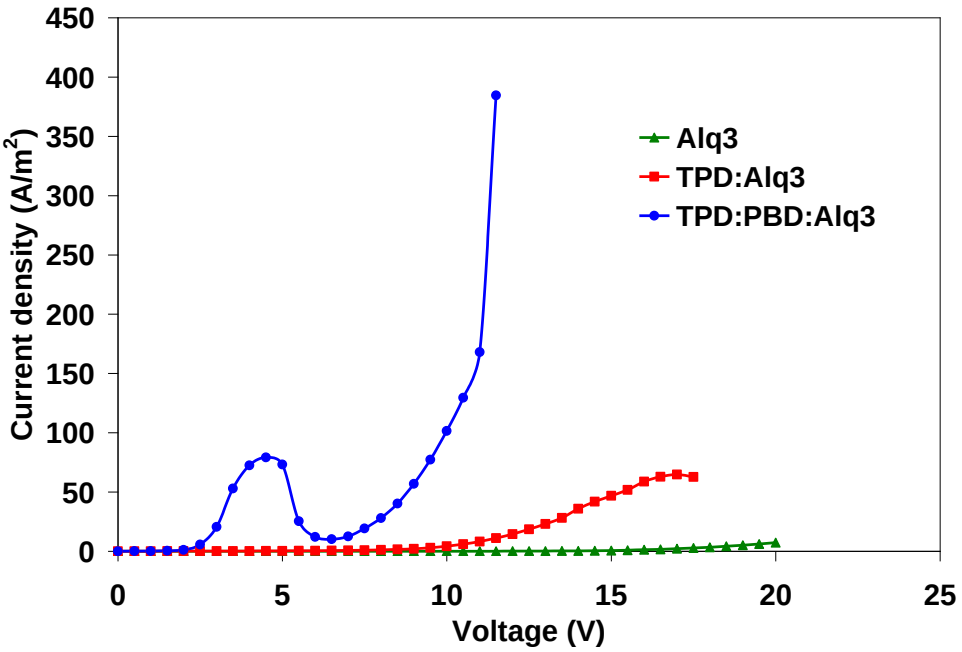

Figure 5.10: *J-V* characteristic of single layer OLED

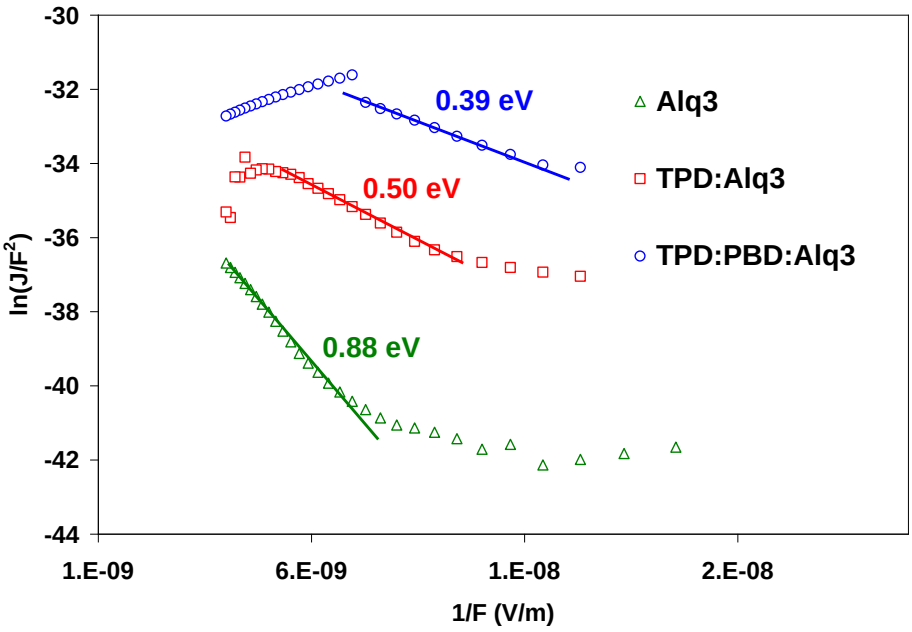

Figure 5.11: F-N plot for devices with different dopant system.

From Fig. 5.10, the anomalous *J-V* characteristic is observed at low driven voltage range from 2.5 to 6 V for TPD:PBD:Alq_3 device which is similarly reported by [*Manca et al., 1998*]. Moreover, the anomalous effect in TPD:Alq_3 blends OLED can be observed by plotting the *J-V* characteristic on a logarithmic scale [*Berleb et al., 1999*] as shown in Fig. 5.12. This feature is called negative differential resistance (NDR). It has been discussed that the NDR effect in OLED doped system was related to guest-hopping sites (GHS) and phonon scattering [*Y. K. Fang et al., 2008*]. In addition, it has been reported that molecular doping will generate hopping site in the TPD doped system [*W. J. Lee, Fang, Chiang, Ting, Chen, Chang, Lin, Lin, & Ho*, 2003]. The same argument has been discussed for OLEDs base on NPD/poly-Alq_3 blends, which hopping-type bipolar charge transport was considered [*Y. S. Kim et al., 2008*]. Thus, it is suggested that GHS was formed in the TPD:PBD:Alq_3 OLED system.

Fig. 5.12 illustrates how the *J* and *V* can be related with such power laws of $J \sim V^m$, where *m* is the magnitude of differential resistant. For the pure Alq_3, the device exhibits clearly three transporting regions; ohmic, space-charge limited current (SCLC) and trap charge limited current (TCLC) with the value of *m* as 1.9, 4.7 and 9.1, respectively. For TPD:Alq_3 device, the current density obtained is higher as compared to that of the pure Alq_3 device, however it exhibits a slight drop in the current value with -1.0 value of *m*. This is where the NDR phenomena occur. For the TPD:PBD:Alq_3 device, the NDR effect is more obvious with a high negative value of m=-4. Fig. 5.13 shows a schematic diagram of carrier pathways in TPD:PBD:Alq_3 blends OLEDs. In a very low voltage region (0 to 2 V), holes and electrons are injected from anode and cathode, respectively, and travel through GHS. More injection at a higher bias (2.5 to 4.5 V) results in a rapid current rise. After 4.5 V of bias, the holes and electrons are still travelling through GHS, however, at the same time, they recombine at the Alq_3

molecule to generate phonons. These energetic phonons then scatter the carriers to decrease the mobility and current, simultaneously [*Nan et al., 2009*], which result in NDR phenomenon. This behavior is not observed in the very low bias indicating that the number of generated phonons is too small to affect the mobility of the carriers. For bias above 6 V, the applied electric field is sufficient enough to facilitate the transportation of holes and electrons through HOMO level of TPD and LUMO level of PBD, respectively. The recombination of carriers was then occurring in the Alq_3 molecule (from LUMO to HOMO level of Alq_3) to release photon energy as an emission. High amount of phonons in the system also explains the rapid Joule heating process in such a blend OLED. It is postulated that the generation of GHS is an important feature that cause the reduction in the effective barrier height where injection mechanism is enhanced.

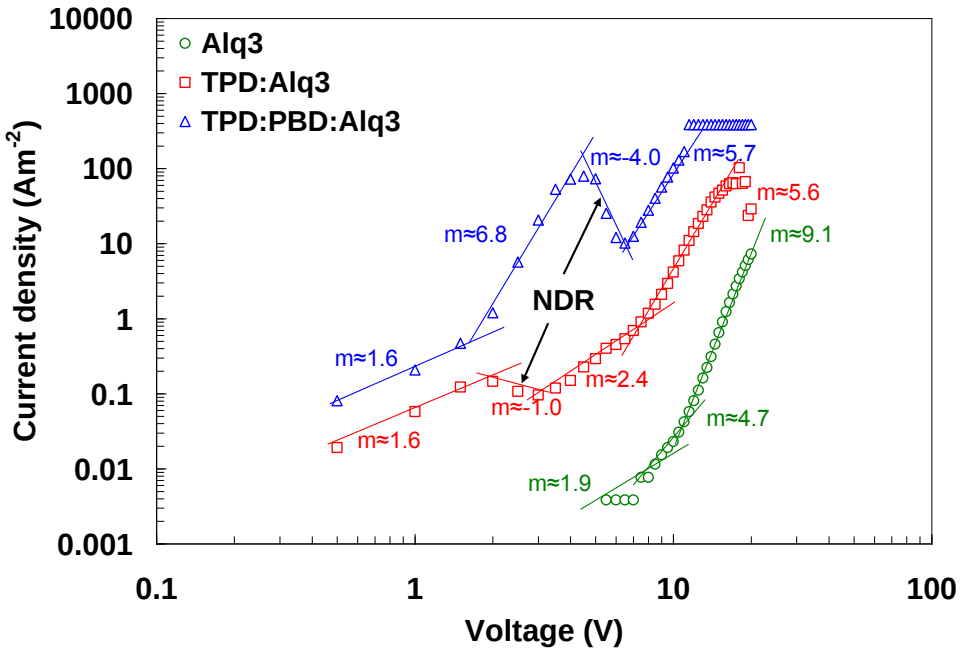

Figure 5.12: *Log J-Log V* plot of single layer OLED

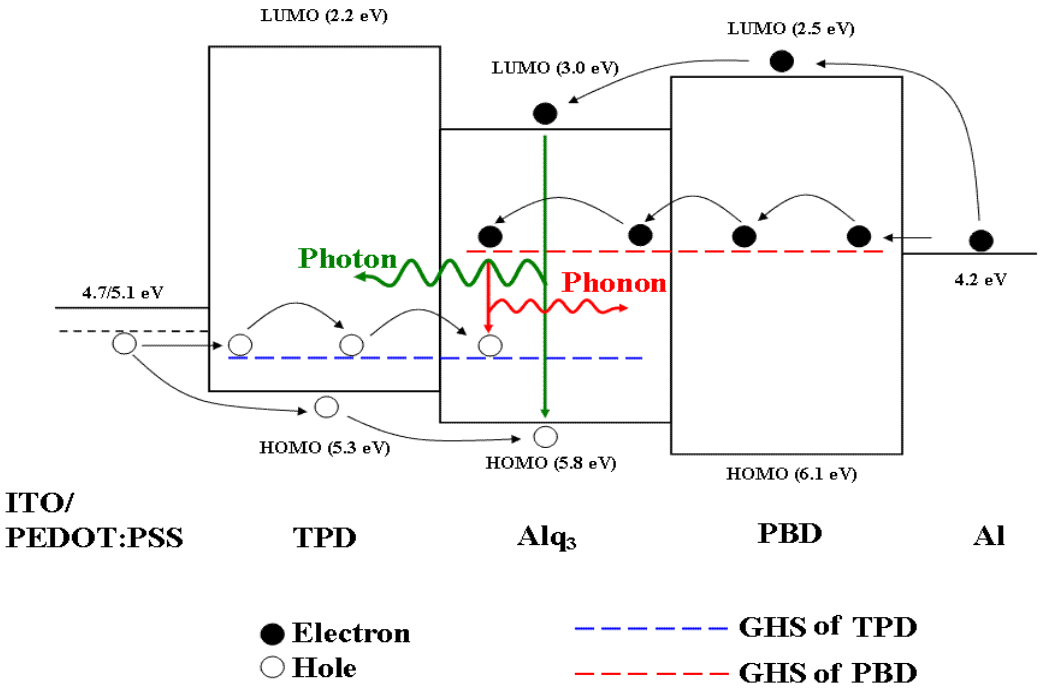

Figure 5.13: Schematic diagram of carrier pathways in TPD:PBD:Alq_3 OLED

Luminance of the single layer OLED was observed to increase by introducing the dopant molecule in Alq_3 based OLED. Fig. 5.14 shows the luminance intensity with respect to driven voltage supplied to the OLED device with different blend system. The significant improve in the turn-on voltage (when L=1 cd/m^2) was obtained for TPD:PBD:Alq_3 blend (5 V) as compared to that of the pure Alq_3 device (15 V). The maximum luminance (before the voltage drops due to Joule heating) was significantly improves from 8±1 cd/m^2 for Alq_3 OLED up to 347±10 cd/m^2 for TPD:PBD:Alq_3 blend OLED. The percentage of increment is calculated to be 41.7 %. In TPD:PBD:Alq_3 based OLED, the Alq_3 molecule is acts as a luminescence center which has been proven by PL result as discussed in the previous section. On the other hand, TPD and PBD act as a hole transporting and an electron transporting dopant, respectively. Thus, the amount of charge carriers (hole and electron) that were injected into the organic layer was much more balanced as compared to other OLEDs. The accumulation of the balance charge carriers creates more exciton. More recombination of the exciton occurs

due to the Coulomb interaction, in which resulting in the significant increase in luminance of the OLED device. The current efficiency, η can be directly understood as the ratio of luminance, L (cd/m^2) emitted with respect to the amount of current density applied, J (A/m^2). A maximum η is obtained to be increased from 1.1±0.2 cd/A for Alq_3 to 2.7±0.7 cd/A for TPD:PBD:Alq_3 OLEDs. The increase in the current efficiency indicated that the TPD and PBD played an important role in facilitating the enhancement of the exciton formation by trapping and transporting more carriers inside the Alq_3 emissive molecule.

Luminescent of OLED depends on an amount of radiative recombination of exciton. Thus it is important to study the relation between carriers accumulation with the dopant system in the device that results in the high luminescent device. Fig. 5.15 shows luminance-current density (*L*-*J*) characteristic of the fabricated OLED with different dopant systems. Current density at the turn on voltage of the devices was observed to increase from 0.9 to 35.5 A/m^2 when the TPD and PBD dopants are blended into Alq_3 emissive layer. The turn on current was supposed to reduce due to the improvement on the injection and transportation of the blend OLED. Turn on current is referred as the value of current where the luminance of the devices is 1 cd/m^2. For TPD:Alq_3 OLED, holes are transporting with high mobility as compared to electron, when TPD is introduced in Alq_3 molecule. The configuration of TPD:Alq_3 OLED is referred as hole only device in which the hole more easily been injected from anode as compared to injection of electron from cathode, due to such a low injection barrier of hole. This may leads to unbalance electron-hole recombination in such a blend which result in slight increase of the turn on current of the device. However, different approach need to be considered for TPD:PBD:Alq_3 device. A high turn on current indicates that the recombination of exciton from GHS release phonon energy that leads to non-

radiative emission. A high current density at a low voltage is attributed from the efficient transportation of charge carrier through GHS.

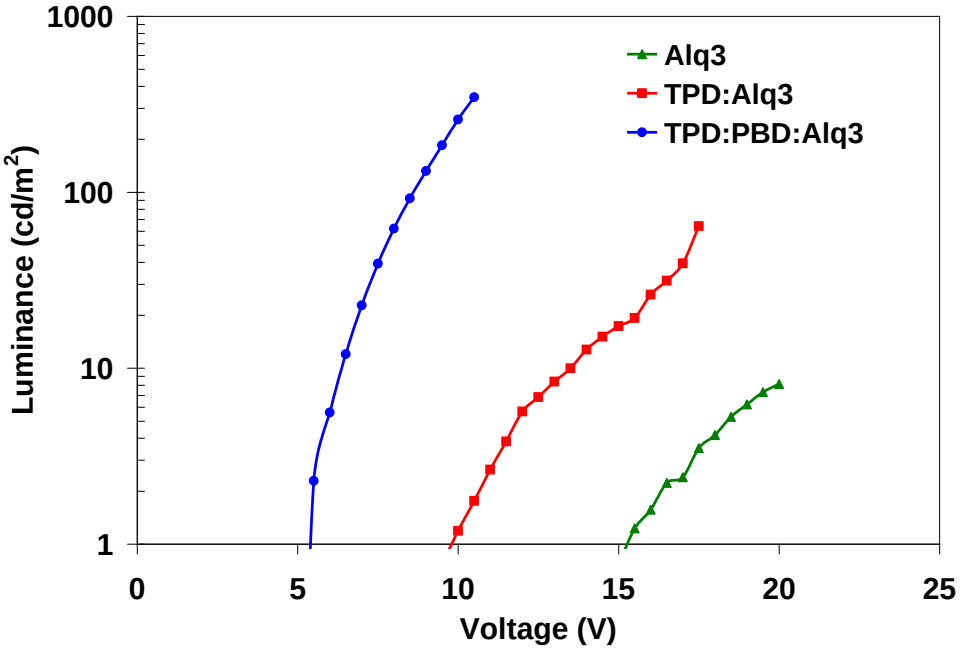

Figure 5.14: L-V characteristic of single layer OLED

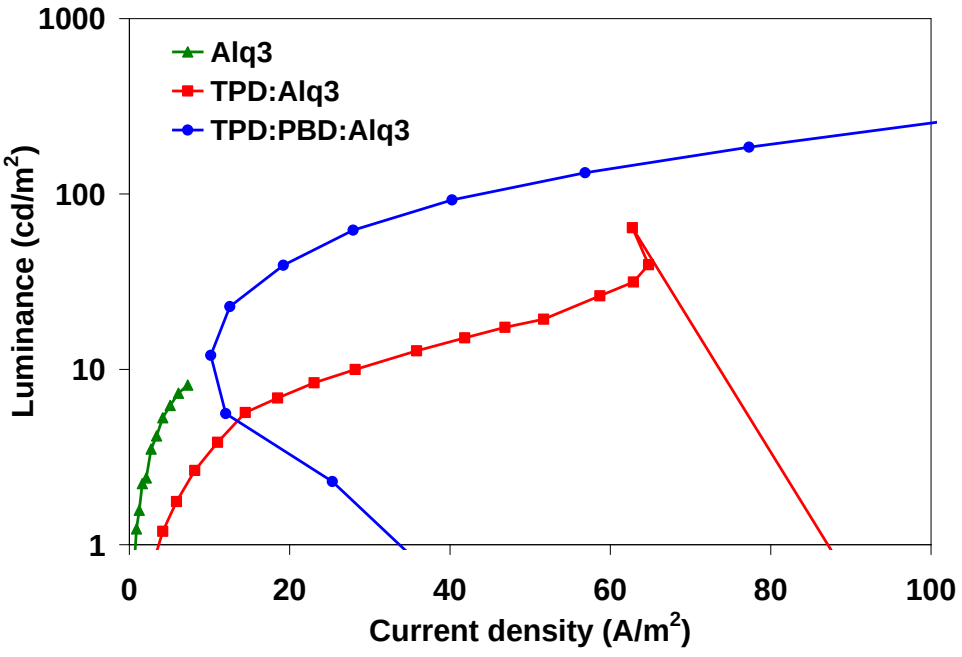

Figure 5.15: Luminance-current characteristic of single layer OLED

Beside the luminance data, the *Commission Internationale de l'Eclairage* or CIE coordinate of emitted light is also recorded. Fig. 5.16 shows CIE plot of the single layer blend OLEDs. The emission of light from all the blend OLEDs were observed within green light region. Interestingly, the CIE coordinates were shifted toward the higher value of x-axis and downward to the lower value of y-axis. This shift phenomena indicates that there are small change in color tone from pure green towards yellowish-green when the Alq_3 based OLED was doped with the hole transporting and the electron transporting molecules. These results can also correlate with the PL results where the PL emission for all the blend system was green. However the PL result doesn't show the shift phenomena probably due to the excitation energy that has been used is not suitable to detect the small change in the PL peak. The summary of the single layer OLEDs performance are shown in Table 5.2.

Fig. 5.17 shows the current efficiency-voltage characteristic of such blends OLED. As has been expected, TPD:PBD:Alq_3 OLED gives the highest current efficiency as compared to the other systems. Even though the luminance result shows TPD:Alq_3 gives more intense luminance as compared to Alq_3 OLED, however, due to relatively high current density obtained in TPD:Alq_3 OLED makes the current efficiency of the device lower as compared to Alq_3 OLED. The current efficiency was taken from the highest luminance which is referred as the maximum current efficiency.

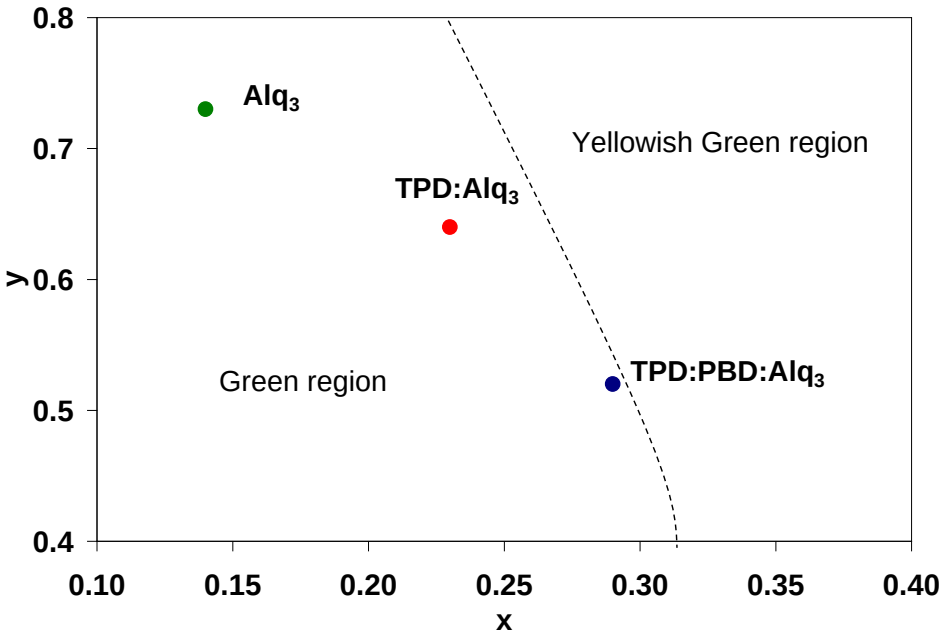

Figure 5.16: CIE plot of single layer OLED

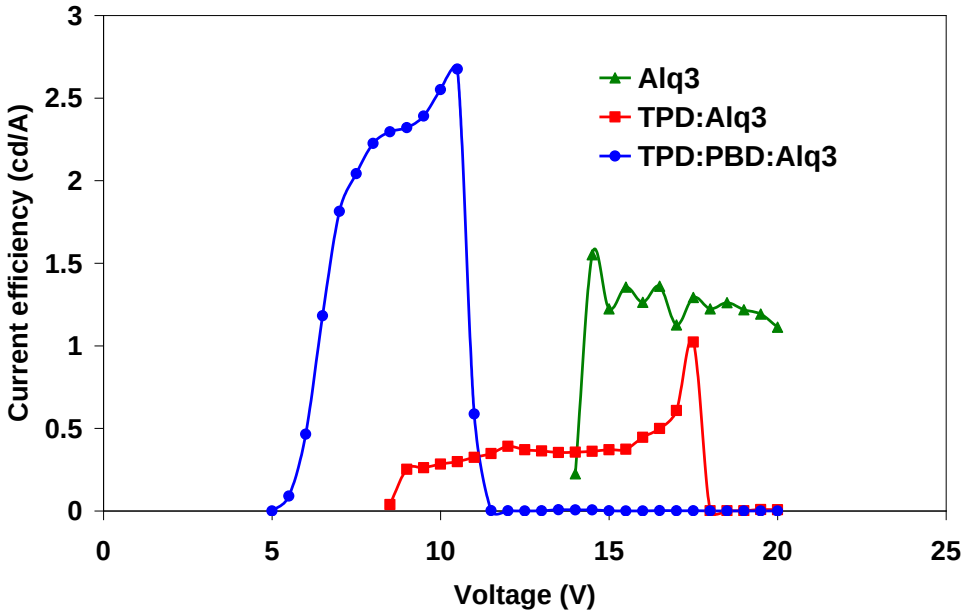

Figure 5.17: Current efficiency-voltage plot of different blends OLED

Table 5.2: Performance of single layer OLED

	Emissive layer		
	Alq_3	TPD:Alq_3	TPD:PBD:Alq_3
V_{on} (±0.5 V)	15.5	10.0	5.0
V_{off} (±0.5 V)	20.0	17.5	11.5
J_{max} (±0.2 A/m^2)	7.3	62.8	384.6
L_{max} (cd/m^2)	8±1	64±4	347±10
η_{max} (cd/A)	1.1±2	1.0±0.3	2.7±0.7

5.7 Impedance Analysis

Beside I-V measurement, impedance spectroscopy has also been used to show the enhancement of conductivity in the blend OLED device. Fig. 5.18 shows the Cole-Cole plot of the OLED device with different blend systems at zero bias voltage. This kind of experiment has been performed to study the effect of various plasma treatments on the surface of the ITO anode [*Hyungjun Park, 2007*]. It is observed that the radius of Cole-Cole plot was reduced as the number of dopant in the blend system is increased. A significant reduction of TPD:PBD:Alq_3 OLED can clearly been seen in Fig. 5.18(a). These results indicate that the impedance of the device is reduced as the hole and electron transporting molecules are doped together in the emissive molecule. A large displacement for the plot of TPD:Alq_3 from origin is observed which can be associated to the increase of contact resistance. Further analysis is performed to clarify the effects of doping in the emissive molecule by simulation and fitting to the absolute impedance of the devices. The simulated results for the devices are presented as solid lines in Fig. 5.19. The square box is the experimental data and the solid line is the simulation fitting results. The value of parallel resistance (R_p) is reduced from 5×10^5 for Alq_3 OLED to 2.3×10^3 Ω for TPD:PBD:Alq_3 OLED. This reduction result in an increase in the

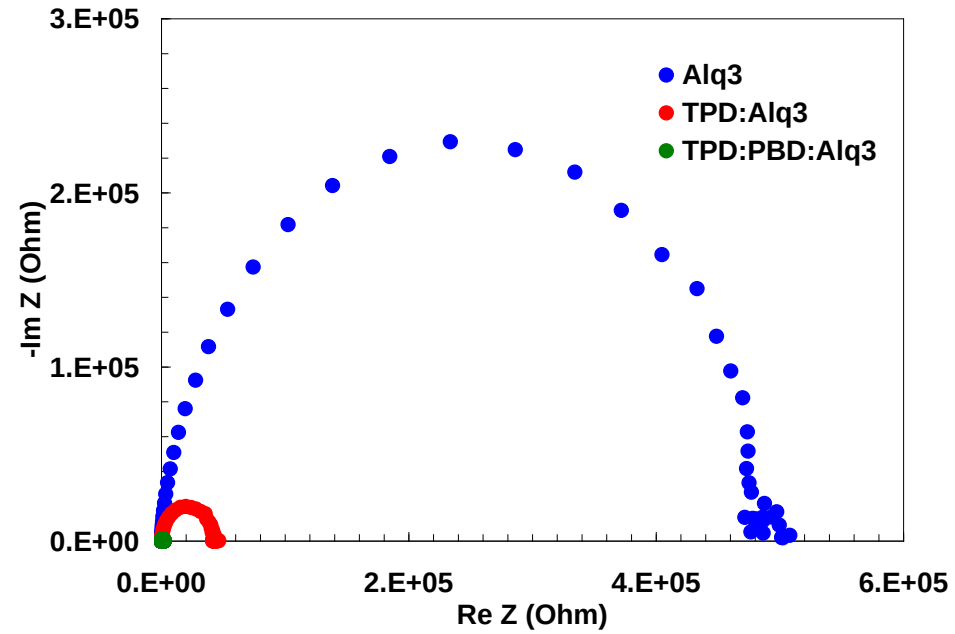

(a)

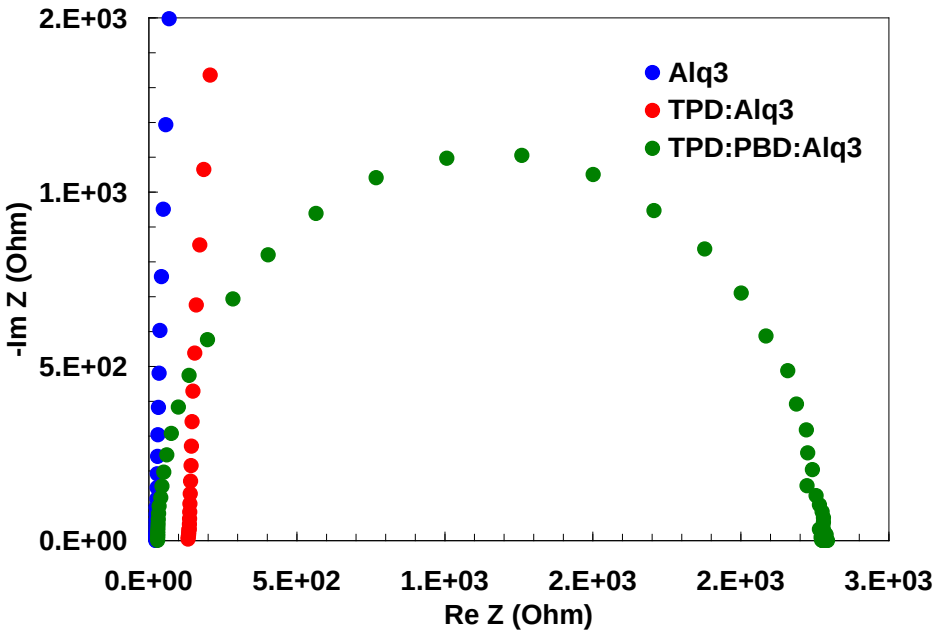

(b)

Figure 5.18: Impedance Cole-Cole plots for OLED fabricated with different blends system at (a) large and (b) smaller scale

effective conductivity (σ_{eff}) up to magnitude of 10^3. This result can be explained by considering the type of dopant molecules. For Alq_3 OLED, the majority charge carrier is electron and by adding with hole transporting molecule of TPD and electron

transporting molecule of PBD, the mobility carrier of the device is increased [*Po-Ching Kao, 2011*]. An efficient transportation of carrier leads to significant reduction in the organic layer resistance. A very minimal reduction of C_p can be neglected and seem to be a constant. Table 5.3 shows the summary of impedance and conductivity parameters for the OLED devices.

Another important feature of impedance analysis is the relaxation time of carrier lifetime. Fig. 5.20(a) shows the overlapping plot of real and imaginary parts of impedance for various blend OLEDs. From Fig. 5.20(a), the value of resonance frequency is observed to shift towards a higher frequency when the number of dopant is increased. In other words, the lifetime of carrier is reduced indicating that the mobility of carrier in OLED device is enhanced by introducing the dopant molecules. The relation between resonance frequency and relaxation time with respect to blends system is shown in Fig. 5.20(b)

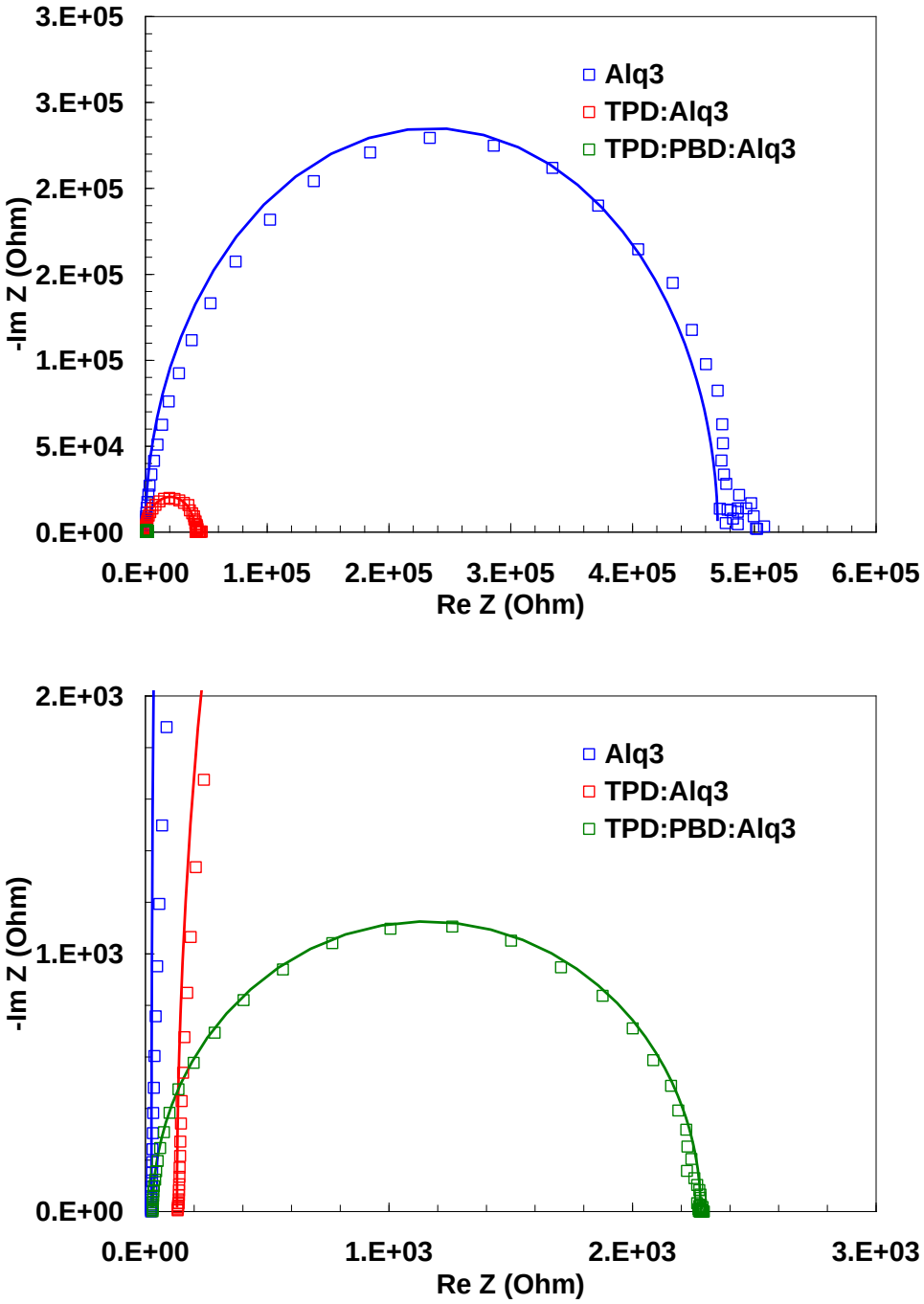

Figure 5.19: Simulated Cole-Cole plots of OLED device fabricated with different blends system at large (above) and low (below) impedance scales.

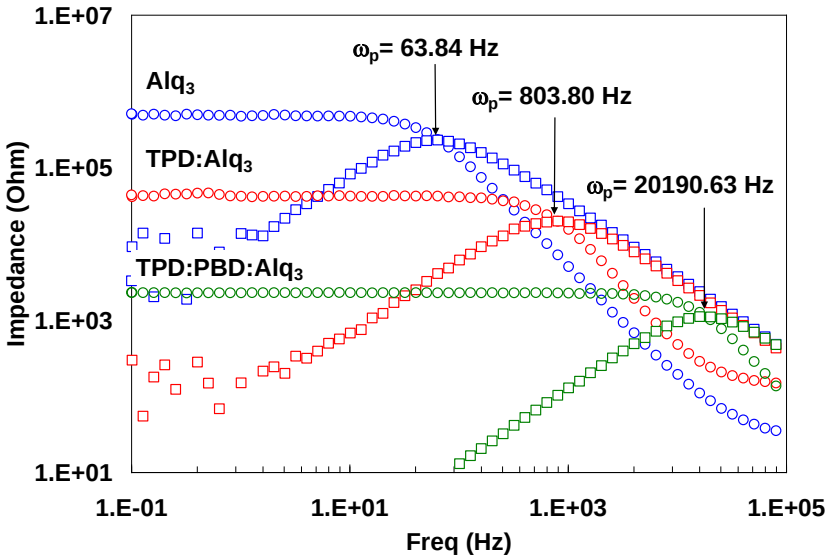

(a)

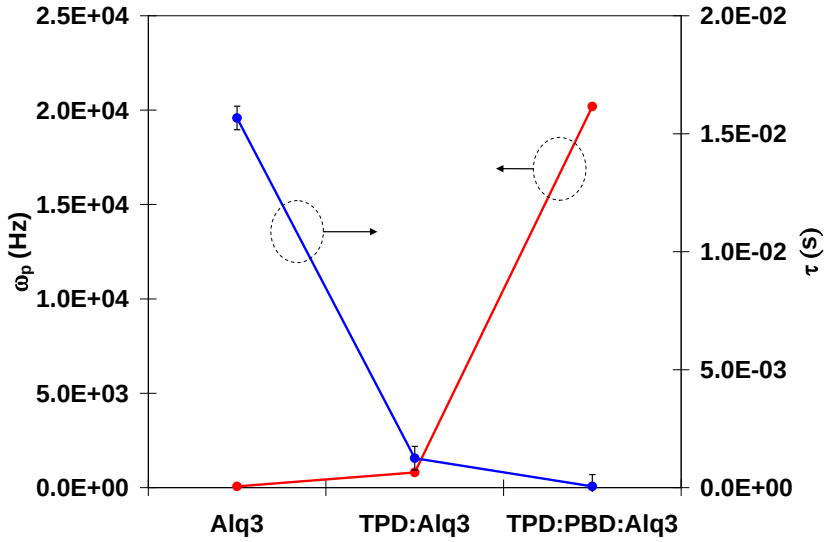

(b)

Figure 5.20: (a) Frequency dependent of real and imaginary part of the impedance and (b) relation between the resonance frequency and the relaxation time of OLED device fabricated with different blends system.

Table 5.3: Impedance parameter used to simulate the measured impedance plot of Fig. 5.19

OLED	R_s (±1 Ω)	R_p (±0.5 Ω)	C_p (±10 nF)	σ_{eff} ($\Omega^{-1}m^{-1}$)
Alq_3	15	5.0×10^{5}	25	$(6\pm2)\times10^{-9}$
TPD:Alq_3	13	4.5×10^{4}	23	$(7\pm3)\times10^{-8}$
TPD:PBD:Alq_3	9	2.3×10^{3}	19	$(1.3\pm0.1)\times10^{-6}$

5.8 Conclusion

Structural, optical and electroluminescence properties of novel blend OLED based on small molecule have been investigated. The FTIR structural studies show that each element of Alq_3, TPD and PBD molecules were remained the same after they were blended together. The XRD pattern confirms that the molecular arrangement of the thin films were amorphous. The optical study indicates that the absorption spectrum of the blends film is obtained from the overlapping absorption spectrum of each element in the blend system. The energy gap of the films increased as the dopants molecules was blended. The PL study shows that the Alq_3 molecule plays an important role as the center of luminance where all the thin film exhibits green emission including the blend one. The PL intensity increased with the increase in the number of dopant molecule due to the improvement in the energy transfer from the dopant to Alq_3. The TPD:PBD:Alq_3 blend OLED exhibits the highest maximum luminance and current efficiency as compared to the other devices which can be related to a more balanced carrier accumulation in the recombination region as hole and electron transporting molecule were blended into Alq_3 molecule. Introducing dopant molecules in Alq_3 single layer OLED also result in the significant reduction in hole barrier height which improves the injection mechanism of hole at anode-organic interface. An anomalous current characteristic was observed in TPD:PBD:Alq_3 OLED where the device exhibits a high

negative differential resistant (NDR) at a low voltage region. The occurrence of NDR is related to the generation of guest hopping side (GHS) and phonon scattering phenomenon. However, the NDR does not alter the luminance and current efficiency of the device at high voltage region. Impedance spectroscopy results clarified the enhancement of mobility carrier by employing the dopant molecules since the highest conductivity is achieved from TPD:PBD:Alq_3 OLED device.

References

Adachi, Chihaya, Tsutsui, Tetsuo, & Saito, Shogo. (1990). Blue light-emitting organic electroluminescent devices. *Applied Physics Letters, 56*, 799-801.

An, Haiyan, Hou, Jingying, Chen, Baijun, Shen, Jiacong, & Liu, Shiyong. (1998). Fabrication and characterization of high quality organic multiple quantum well structures. *Thin Solid Films, 326*, 201-204.

Berleb, S., Brütting, W., & Schwoerer, M. (1999). Anomalous current-voltage characteristics in organic light-emitting devices. *Synthetic Metals, 102*, 1034-1037.

Blochwitz, J., Pfeiffer, M., Fritz, T., & Leo, K. (1998). Low voltage organic light emitting diodes featuring doped phthalocyanine as hole transport material. *Applied Physics Letters, 73*, 729-731.

Camurlu, P., Giovanella, U., Bolognesi, A., Botta, C., Cik, G., & Végh, Z. (2009). Polythiophene-polyoxyethylene copolymer in polyfluorene-based polymer blends for light-emitting devices. *Synthetic Metals, 159*, 41-44.

Chopra, Neetu, Lee, Jaewon, Zheng, Ying, Eom, Sang-Hyun, Xue, Jiangeng, & So, Franky. (2008). High efficiency blue phosphorescent organic light-emitting device. *Applied Physics Letters, 93*, 143307-143303.

Cossiello, Rafael F., Cirpan, Ali, Karasz, Frank E., Akcelrud, Leni, & Atvars, Teresa D. Z. (2008). Electroluminescence of (styrene-co-acrylic acid) ionomer/conjugated MEH-PPV blends. *Synthetic Metals, 158*, 219-225.

Costela, Angel, García-Moreno, Inmaculada, Gómez, Clara, García, Olga, Garrido, Leoncio, & Sastre, Roberto. (2004). Highly efficient and stable doped hybrid organic-inorganic materials for solid-state dye lasers. *Chemical Physics Letters, 387*, 496-501.

El-Nahass, M. M., Farid, A. M., & Atta, A. A. (2010). Structural and optical properties of Tris(8-hydroxyquinoline) aluminum (III) (Alq3) thermal evaporated thin films. *Journal of Alloys and Compounds, 507*, 112-119.

Fang, Junfeng, Chan Choy, Chum, Ma, Dongge, & Ou, Eric C. W. (2006). High-efficiency spin-coated organic light-emitting diodes based on a europium complex. *Thin Solid Films, 515*, 2419-2422.

Fang, Y. K., Chiang, Y. T., Chen, S. F., Lin, C. Y., Hou, S. C., Hung, C. S., . . . Chou, T. H. (2008). Observation of room temperature negative differential resistance (NDR) in organic light-emitting diode with inorganic dopant. *Journal of Physics and Chemistry of Solids, 69*, 738-741.

Hebner, T. R., Wu, C. C., Marcy, D., Lu, M. H., & Sturm, J. C. (1998). Ink-jet printing of doped polymers for organic light emitting devices. *Applied Physics Letters, 72*, 519-521.

Hopkins, A. R., Lipeles, R. A., & Kao, W. H. (2004). Electrically conducting polyaniline microtube blends. *Thin Solid Films, 447-448*, 474-480.

Hyungjun Park, Hyunmin Kim, S. K. Dhungel, Junsin Yi. (2007). Impedance Spectroscopy Analysis of Organic Light-Emitting Diodes Fabricated on Plasma-Treated Indium-Tin-Oxide surfaces. *Journal of the Korean Physical Society, 51*, 1011-1015.

Kalinowski, J., & Szybowska, K. (2008). Photoconduction in the archetype organic hole transporting material TPD. *Organic Electronics, 9*, 1032-1039.

Kao, Po-Ching, Lin, Jie-Han, Wang, Jing-Yuan, Yang, Cheng-Hsien, & Chen, Sy-Hann. (2011). Li[sub 2]CO[sub 3] as an n-type dopant on Alq[sub 3]-based organic light emitting devices. *Journal of Applied Physics, 109*, 094505-094506.

Kim, Sung-Jin, Zhang, Yadong, Zuniga, Carlos, Barlow, Stephen, Marder, Seth R., & Kippelen, Bernard. (2011). Efficient green OLED devices with an emissive layer comprised of phosphor-doped carbazole/bis-oxadiazole side-chain polymer blends. *Organic Electronics, 12*, 492-496.

Kim, Y. S., Jung, S. Y., Koh, K. H., Lee, S., & Ko, K. Y. (2008). Electroluminescence of devices fabricated using a soluble Alq3 pendent polymer. *Journal of the Korean Physical Society, 53*, 3563-3567.

Kin, Zenken, Kajii, Hirotake, Hasegawa, Yasuchika, Kawai, Tsuyoshi, & Ohmori, Yutaka. (2008). Optical and electroluminescent properties of samarium complex-based organic light-emitting diodes. *Thin Solid Films, 516*, 2735-2738.

Lee, Cheol Eui, Jang, Jae Won, Lee, Hoo Min, Oh, Dong Keun, Lee, Chang Hoon, Lee, Dong Won, & Jin, Jung-Il. (2001). Charge-carrier mobilities and charge conduction in a poly(p-phenylenevinylene) derivative carrying an electron-transporting moiety. *Current Applied Physics, 1*, 107-111.

Lee, D. H., Choi, J. S., Chae, H., Chung, C. H., & Cho, S. M. (2009). Screen-printed white OLED based on polystyrene as a host polymer. *Current Applied Physics, 9*, 161-164.

Lee, Joo-Hyeon, Kim, Sun-Woong, Ju, Sung-Hoo, Lee, Won-Geun, Choi, Jong-Sun, Kim, Young-Kwan, & Kim, Woo Young. (2000). Emission shift by recombination effect in a three-layered oeld. *Synthetic Metals, 111-112*, 63-67.

Lee, W. J., Fang, Y. K., Chiang, H. C., Ting, S. F., Chen, S. F., Chang, W. R., . . . Ho, J. J. (2003). Dramatic improving luminous efficiency of organic light emitting diodes under low driving current using nitrogen doped hole transporter. *Solid-State Electronics, 47*, 1127-1130.

Lee, W. J., Fang, Y. K., Chiang, Hsin-Che, Ting, S. F., Chen, S. F., Chang, W. R., . . . Ho, Jyh-Jier. (2003). Improving turn on voltage and driving voltage of organic electroluminescent devices with nitrogen doped electron transporter. *Solid-State Electronics, 47*, 927-929.

Madasamy, S., Pavicic, D., Rothe, C., Murano, S., Birnstock, J., Blochwitz-Nimoth, J., . . . Pfeiffer, M. (2008). *An overview about the use of electrical doping of charge carrier transport layers in OLEDs and further organic electronic applications*.

Manca, J., Bijnens, W., Kiebooms, R., D'Haen, J., D'Olieslaeger, M., Wu, T. D., . . . Stals, L. (1998). Effect of oxygen on the electrical characteristics of PPV-LEDs. *Optical Materials, 9*, 134-137.

Nan, Guangjun, Yang, Xiaodi, Wang, Linjun, Shuai, Zhigang, & Zhao, Yi. (2009). Nuclear tunneling effects of charge transport in rubrene, tetracene, and pentacene. *Physical Review B, 79*, 115203.

Neghabi, Mina, & Behjat, Abbas. (2012). Electrical and electroluminescence properties of ITO/PEDOT:PSS/TPD:Alq3:C60/Al organic light emitting diodes. *Current Applied Physics, 12*, 597-601.

Nie, H., Zhang, B., & Tang, X. Z. (2007). Significant improvement of OLED efficiency and stability by doping both HTL and ETL with different dopant in heterojunction of polymer/small-molecules. *Chinese Physics, 16*, 730-734.

Paul, P. K., Hussain, S. A., & Bhattacharjee, D. (2008). Photophysical characterizations of 2-(4-biphenylyl)-5 phenyl-1,3,4-oxadiazole in restricted geometry. *Journal of Luminescence, 128*, 41-50.

Po-Ching Kao, Jie-Han Lin, Jing-Yuan Wang, Cheng-Hsien Yang, Sy-Hann Chen. (2011). Li2CO3 as an n-type dopant on Alq3-based organic light emitting devices. *Journal of Applied Physics, 109*, 094505-094501-094505.

Reyes, R., Cremona, M., Teotonio, E. E. S., Brito, H. F., & Malta, O. L. (2004). Voltage color tunable OLED with (Sm,Eu)-[beta]-diketonate complex blend. *Chemical Physics Letters, 396*, 54-58.

Shih, Chuan-Feng, Hung, Kuang-Teng, Chen, Hui-Ju, Hsiao, Chu-Yun, Huang, Kuan-Ta, & Chen, Szu-Hung. (2011). Incorporation of potassium at CuPc/C[sub 60] interface for photovoltaic application. *Applied Physics Letters, 98*, 113307-113303.

Tsuboi, T., Bansal, A. K., & Penzkofer, A. (2009). Fluorescence and phosphorescence behavior of TPD doped and TPD neat films. *Thin Solid Films, 518*, 835-838.

Valadares, M., Silvestre, I., Calado, H. D. R., Neves, B. R. A., Guimarães, P. S. S., & Cury, L. A. (2009). BEHP-PPV and P3HT blends for light emitting devices. *Materials Science and Engineering: C, 29*, 571-574.

Vragović, I., Calzado, E. M., Díaz García, M. A., Himcinschi, C., Gisslén, L., & Scholz, R. (2008). Modelling absorption and photoluminescence of TPD. *Journal of Luminescence, 128*, 845-847.

Xie, Guohua, Meng, Yanlong, Wu, Fengmin, Tao, Chen, Zhang, Dandan, Liu, Mingjun, . . . Zhao, Yi. (2008). Very low turn-on voltage and high brightness tris-(8-hydroxyquinoline) aluminum-based organic light-emitting diodes with a MoOx p-doping layer. *Applied Physics Letters, 92*, 093305-093305-093303.

Xu, S., Yang, M., & Cao, S. (2006). A fluorescent copolyimide containing perylene, fluorene and oxadiazole units in the main chain. *Reactive and Functional Polymers, 66*, 471-478.

Yap, C. C., Yahaya, M., & Salleh, M. M. (2008). Influence of thickness of functional layer on performance of organic salt-doped OLED with ITO/PVK:PBD:TBAPF6/Al structure. *Current Applied Physics, 8*, 637-644.

Yap, C. C., Yahaya, M., & Salleh, M. M. (2009). Influence of tetrabutylammonium hexafluorophosphate (TBAPF6) doping level on the performance of organic light emitting diodes based on PVK:PBD blend films. *Current Applied Physics, 9*, 722-726.

Zhang, T., Xu, Z., Qian, L., Teng, F., Xu, X. R., & Tao, D. L. (2005). Improved emission of Eu3+ by energy transfer via Tb3+ in coprecipitates TbxEu(1-x)aspirin3(phen). *Journal of Applied Physics, 98*, 063503-063503-063504.